

[CASE REPORT]

Pancreatic Neuroendocrine Neoplasm Invading the Entire Main Pancreatic Duct Diagnosed by a Preoperative Endoscopic Biopsy

Tomoya Kimura¹, Mitsuru Sugimoto¹, Tadayuki Takagi¹, Rei Suzuki¹, Naoki Konno¹, Hiroyuki Asama¹, Yuki Sato¹, Hiroki Irie¹, Jun Nakamura^{1,2}, Mika Takasumi¹, Minami Hashimoto^{1,2}, Tsunetaka Kato¹, Yasuhide Kofunato³, Takashi Kimura³, Shoki Yamada⁴, Yuko Hashimoto⁴, Shigeru Marubashi³, Takuto Hikichi² and Hiromasa Ohira¹

Abstract:

A 78-year-old man was referred to our hospital for a detailed examination of a pancreatic tumor that filled the main pancreatic duct (MPD). The histological diagnosis of the endoscopic biopsy specimen was neuroendocrine tumor (NET) G3. The patient subsequently underwent total pancreatectomy. The histological diagnosis of the surgical specimen was also NET G3. This is the first report of a NET that occupied the MPD and was diagnosed by a preoperative endoscopic biopsy through the papilla of Vater. This case is a good example of a histopathological diagnostic method for pancreatic tumors invading the entire MPD.

Key words: pancreatic neuroendocrine tumor, main pancreatic duct

(Intern Med 59: 1991-1996, 2020)

(DOI: 10.2169/internalmedicine.4546-20)

Introduction

Neuroendocrine neoplasms (NENs) arise from neuroendocrine cells that exist throughout the body. Pancreatic NENs (PNENs) are rare, accounting for 2-5% of all pancreatic tumors (1). As imaging and diagnostic methods have advanced, an increasing number of cases have been reported recently. In general, PNENs show expansive growth and are characterized by oval-shaped tumor cells, with a clear boundary between the tumor and the pancreatic parenchyma. PNENs rarely invade the main pancreatic duct (MPD).

We herein report a rare case of a PNEN that invaded the MPD and occupied the entire MPD, as diagnosed by a preoperative endoscopic biopsy.

Case Report

A 78-year-old man visited a local doctor for weight loss and abdominal pain. His weight loss had begun one month before he visited the hospital. He underwent computed tomography (CT), which revealed a pancreatic tumor that had expanded and occupied the main pancreatic duct (MPD). He was referred to our hospital for a detailed examination and intensive treatment.

At the first visit, his abdominal pain had improved, and his bowel sounds were normal. There was no palpable abdominal tumor. The results of blood tests indicated normal levels of hepatobiliary enzymes, and no elevated tumor markers were noted (Table 1).

According to transabdominal ultrasonography, the dilated MPD was occupied by a diffuse low-echoic tumor (Fig. 1A). Contrast-enhanced CT revealed that the diameter

¹Department of Gastroenterology, School of Medicine, Fukushima Medical University, Japan, ²Department of Endoscopy, Fukushima Medical University Hospital, Japan, ³Department of Hepato-Biliary-Pancreatic and Transplant Surgery, School of Medicine, Fukushima Medical University, Japan and ⁴Department of Diagnostic Pathology, School of Medicine, Fukushima Medical University, Japan

Received: February 1, 2020; Accepted: March 27, 2020; Advance Publication by J-STAGE: May 23, 2020

Correspondence to Dr. Mitsuru Sugimoto, kita335@fmu.ac.jp

Table 1. Laboratory Data from This Case.

Variable	Value	Units
Hematologic test		
White blood cells	4,700	/ μ L
Neutrophils	40	%
Lymphocytes	40	%
Monocytes	5	%
Eosinophils	13	%
Basophils	2	%
Red blood cells	426 \times 10 ⁴	/ μ L
Hemoglobin	13.6	g/dL
Platelet count	193 \times 10 ⁴	/ μ L
Coagulation		
PT	88.5	%
APTT	32.1	s
Chemistry		
AST	23	U/L
ALT	24	U/L
LD	196	U/L
ALP	283	U/L
γ -GTP	27	U/L
Total bilirubin	0.9	mg/dL
Amylase	68	U/L
Total protein	6.9	g/dL
Albumin	4.1	g/dL
BUN	8	mg/dL
Creatinine	0.88	mg/dL
Sodium	140	mmol/L
Potassium	3.7	mmol/L
Chloride	104	mmol/L
CRP	0.05	mg/dL
Glucose	104	mg/dL
Hemoglobin A1c	6.3	%
Alpha fetoprotein	14.6	ng/mL
Carcinoembryonic antigen	1.8	ng/mL
Carbohydrate antigen 19-9	9.7	U/mL
HBs-Ag	(-)	
HCV-Ag	(-)	

PT: prothrombin time, APTT: activated partial thromboplastin time, AST: aspartate transaminase, ALT: alanine transaminase, LD: lactate dehydrogenase, ALP: alkaline phosphatase, γ GTP: γ -glutamyltransferase, BUN: blood urea nitrogen

of the MPD was 9 mm and that a poorly enhanced tumor fully occupied it (Fig. 1B). The entire tumor in the MPD showed high intensity on diffusion-weighted magnetic resonance imaging (MRI) (Fig. 1C). The low-echoic tumor was detected via endoscopic ultrasonography as well as other imaging modalities (Fig. 1D). The pancreatic parenchyma appeared to be thinning, and the border between the tumor in the MPD and the pancreatic parenchyma was unclear. Therefore, endoscopic ultrasonography-guided fine-needle aspiration (EUS-FNA) was not performed, and it was difficult to determine the main location of the tumor. Endoscopic retrograde cholangiopancreatography (ERCP) indicated that the MPD was dilated with translucency. An endo-

scopic biopsy was performed through the papilla of Vater (Fig. 1E) using Radial Jaw™ 4 Biopsy Forceps (Boston Scientific Japan, Tokyo, Japan). Fluorodeoxyglucose-positron emission tomography (FDG-PET) revealed an abnormal uptake [maximum standardized uptake value (SUV_{max}): 20.1] by the pancreatic head (Fig. 1F), although no clear metastatic lesions were found by FDG-PET.

The pathological results for the endoscopic biopsy showed alveolar structures of atypical cells with minute chromatin (Fig. 2A). These tumor cells were positive for chromogranin A (DAKO, Glostrup, Denmark) (Fig. 2B) and synaptophysin (DAKO) (Fig. 2C) and negative for CD56 (ZYMED, Carlsbad, USA) by immunostaining, and the Ki-67 (DAKO) labeling index was 60%. The histological diagnosis was pancreatic neuroendocrine tumor (PNET) G3 according to the 2019 World Health Organization (WHO) classification (Fig. 2D).

One month after the diagnosis, total pancreatectomy was performed because several preoperative examinations had shown that the tumor affected the entire pancreas. The tumor was white in color, was primarily located in the pancreatic head (Fig. 3A), and grew along the MPD (Fig. 3B). The final diagnosis was similar to the diagnosis based on the endoscopic biopsy. Oval-shaped tumor cells exhibited elevated minute chromatin, with alveolar, rosette, and tubular ductal structures (Fig. 4A). The tumor cells were positive for chromogranin A (DAKO) (Fig. 4B) and synaptophysin (DAKO) (Fig. 4C) and negative for CD56 (ZYMED) (Fig. 4D) by immunostaining. The Ki-67 (DAKO) labeling index was 70-80%, and the mitotic count was 48/10 high-power fields. The histological diagnosis was PNET G3, and the pStage was IB (pT2N0M0).

Two months after surgery, no recurrence or metastatic lesions were observed by contrast-enhanced CT. The patient was then referred to another hospital for further follow-up examinations.

Discussion

Pancreatic tumors with MPD invasion are 1) lesions that show expansive growth (acinar cell carcinoma, adenosquamous cell carcinoma, PNEN, anaplastic cell carcinoma) and 2) intraductal lesions (intraductal papillary mucinous neoplasm main duct type, intraductal tubulopapillary neoplasm) (2-7). Tumors with MPD invasion exhibit various forms, and an acinar cell carcinoma case resembling this one was reported in a previous study (2). As a definitive diagnosis using only imaging modalities is difficult, a histopathological diagnosis is needed. In the present case, a biopsy through the papilla of Vater was performed because of the risk of tumor cell seeding. For cases in which surgery cannot be performed, chemotherapy is administered to both PNEN patients and those with other pancreatic tumors. However, the regimen administered to PNEN patients is different from that administered to other patients, so the differential diagnosis between PNEN and other pancreatic tumors

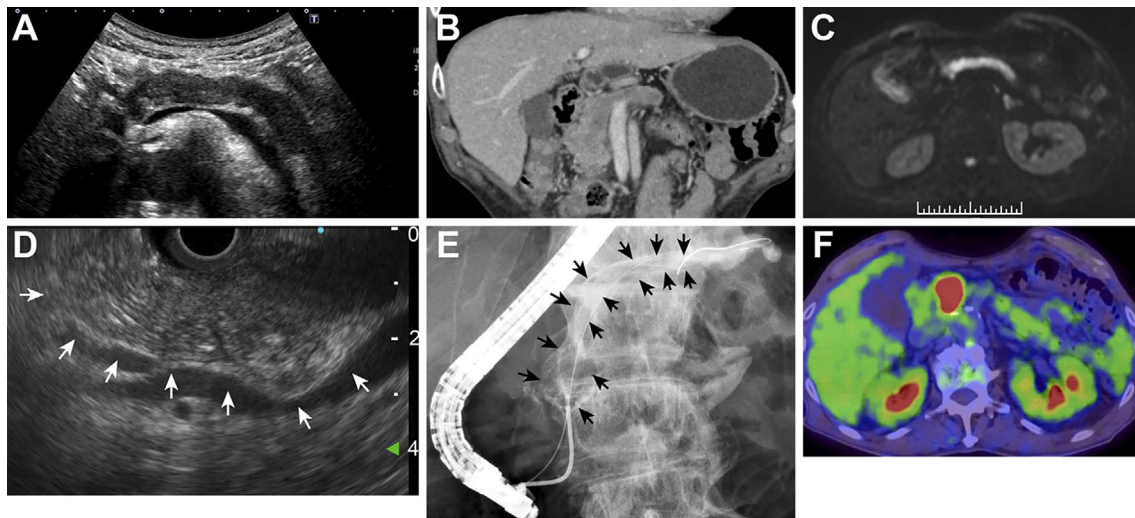


Figure 1. Imaging examinations for this case. A: Abdominal echography showed a dilated MPD occupied by a low-echoic tumor. B: Abdominal contrast-enhanced CT also revealed a dilated MPD. The MPD was occupied by a mildly enhanced tumor. C: The tumor that was detected by abdominal echography and CT exhibited a high intensity on diffusion-weighted MRI. D: Endoscopic ultrasonography showed a dilated MPD of no more than 10 mm. The hypoechoic tumor occupied the pancreatic duct. E: On endoscopic retrograde pancreatography, the area surrounding the tumor was enhanced (arrowheads). A tumor biopsy was performed. F: PET showed an abnormal uptake (SUV_{max} 20.1) by the pancreatic head. MPD: main pancreatic duct, PET: positron emission tomography, SUV_{max} : maximum standardized uptake value

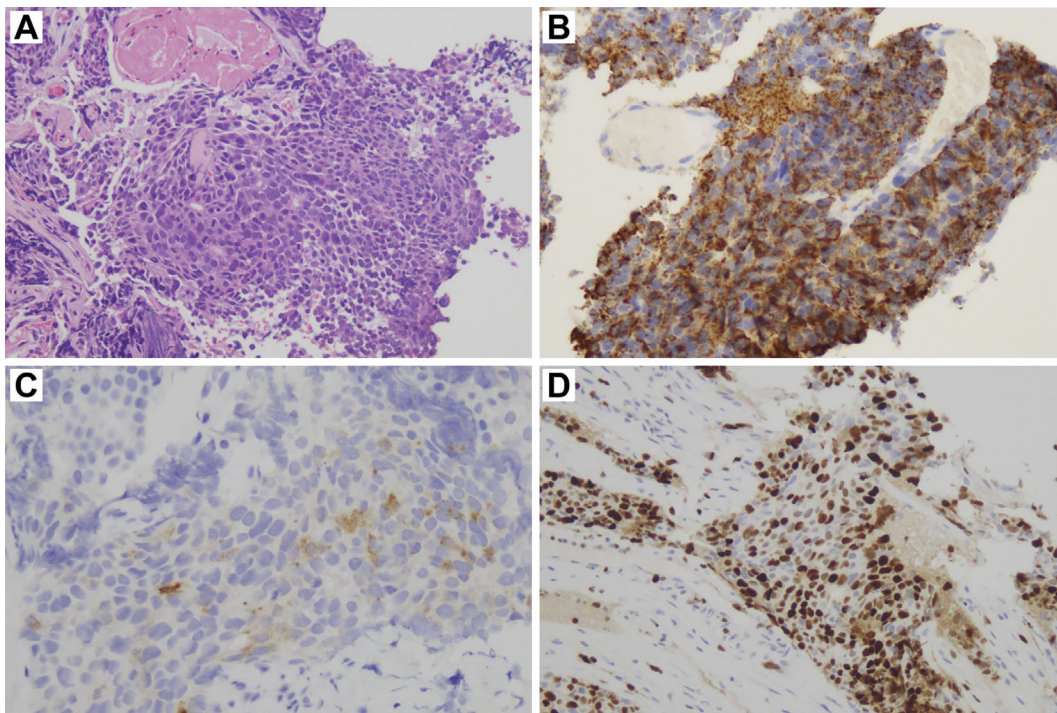


Figure 2. The pathological findings of the endoscopic biopsy. A: Atypical cells showed elevated minute chromatin and the development of alveolar structures. B: The atypical cells were positive for chromogranin A and C: synaptophysin. D: The Ki-67 index was 60%. The histological diagnosis was PNET G3. PNET: pancreatic neuroendocrine tumor

is important. In contrast to previous cases of PNENs with intraductal growth, this case is the first to be diagnosed by a preoperative endoscopic biopsy through the papilla of Vater.

This case report may provide a good example of how to histologically diagnose tumors that fill the MPD.

To our knowledge, only eight PNEN cases with intraduc-

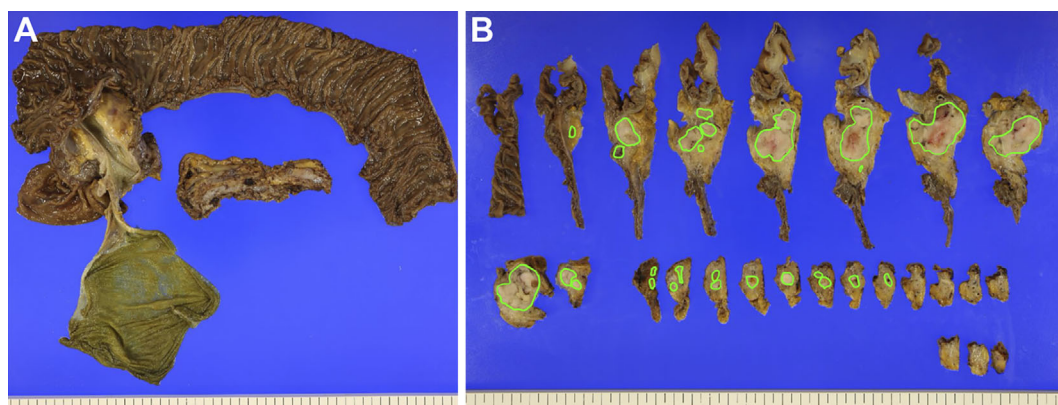


Figure 3. Macroscopic findings from surgery. A: The tumor was mainly located in the pancreatic head. B: The tumor advanced along the MPD. The tumor occupied the area surrounded by the green line. MPD: main pancreatic duct

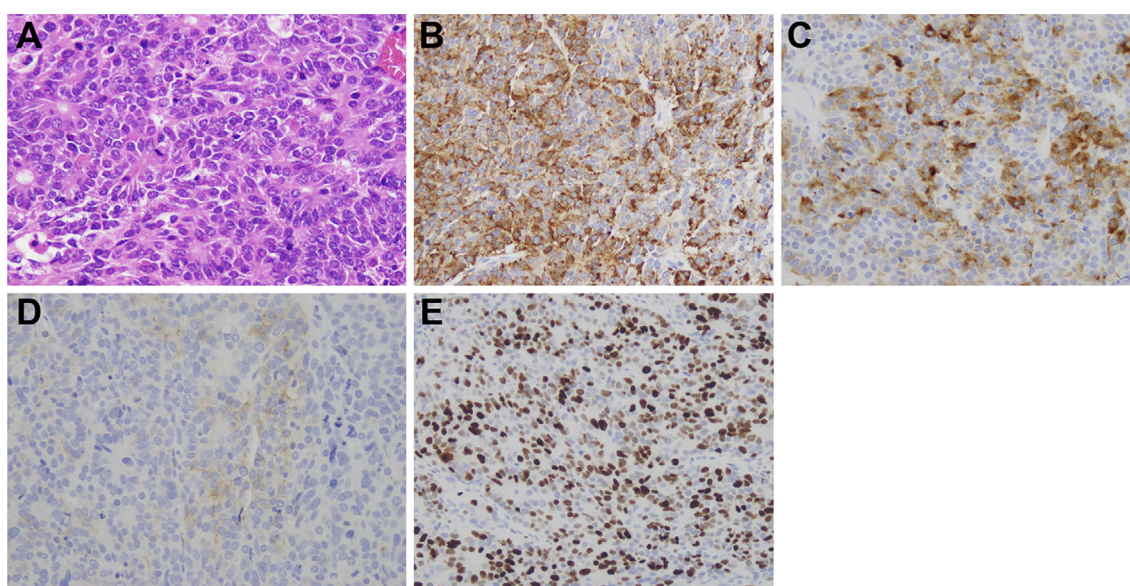


Figure 4. The pathologic findings of the surgical specimen. A: Oval-shaped tumor cells showed elevated minute chromatin and the development of alveolar, rosette and tubular ductal structures. The mitotic count was 48/10 HPFs. B: The tumor cells were positive for chromogranin, C: synaptophysin, and D: CD56. E: The Ki-67 index was 70-80%. The final diagnosis was PNET G3. HPF: high power field, PNET: pancreatic neuroendocrine tumor

tal growth have been reported (8-15). A summary of these eight cases along with the present case is shown in Table 2. NENs of digestive organs are classified as G1, G2, G3 or neuroendocrine carcinoma (NEC) G3 by the 2019 WHO classification based on the cellular proliferative potential (the Ki-67 index and mitotic count) (16), although the previous eight cases were not classified according to the 2019 WHO classification. Six cases were diagnosed as malignant tumors, and one case reported by Yazawa et al. (13) was diagnosed as NEC. One case reported by Kiyonaga et al. (15) was diagnosed as NET G2. Among all grades of NETs, the prognosis of G1 tumors is very favorable. Indeed, the 2-year progression-free survival rate for NET G1 is reported to be 92% (17), with a 2-year survival rate of 100% (18). Although the 5-year survival rate is 82.6% according to Yang

et al. (19) and 55.7% according to Zeng et al. (20), the 5-year survival rate is 90% or higher in other reports (18, 21-24). Nonetheless, previous case reports likely did not include NET G1 patients. As described above, PNETs are surrounded by a fibrous capsule and show expansive growth. In contrast, PNETs with a high proliferation capacity are reported to exhibit irregular shapes and MPD dilation (25). Indeed, the present case report features a high-grade NET G3 tumor. Some previous reports have investigated the correlation between imaging characteristics and the PNET grade. PNENs are generally enhanced in the early phase on contrast-enhanced CT and MRI (26-29), whereas low enhancement is observed in malignant PNENs (30-33). FDG-PET often reveals an FDG accumulation in cases of malignant or highly proliferative PNENs (34, 35). The pro-

Table 2. Summary of the Previous Nine Cases.

Reference number	Age (years)	Sex	Size (mm)	Location	Biopsy specimen from endoscopy		Surgical specimen			Prognosis
					Ki-67 index (%)	Grade	Ki-67 index (%)	Mitotic count (/10 HPFs)	Grade	
8	44	F	NA	Head	Necrotic tissue		<5	NA	Low-grade malignant	NA
9	57	M	15	Tail	NA		15	NA	Malignant	Survived for 2 years
10	43	M	25	Body	NA		<5	NA	Malignant	Survived for 1 year
11	36	M	16	Head	NA		NA	NA	Malignant	Survived for 6 months
12	68	M	29	Head	NA		NA	NA	Malignant	Died from tumor recurrence in the form of multiple liver metastases 11 months after surgery
13	47	F	75	Head-tail	NA		30-40	NA	NEC	Survived for 2 years
14	46	F	30	Head	NA		Low	Low	NA	NA
15	26	F	NA	Head-body	NA		NA	NA	G2	NA
This case	78	M		Head-tail	60	G3	70-80	48	G3	Referred to another hospital 2 months after surgery

F: female, M: male, NA: not available, NEC: neuroendocrine carcinoma

liferation activity observed in the present case was believed to be high because of the high Ki-67 index. Therefore, the imaging findings in this case are the same as those in previous reports.

The tumor grade between the endoscopic biopsy specimen and the surgical specimen was consistent. Similarly, the concordance rate of the tumor grade between EUS-FNA and the surgical specimen in previous reports was relatively high at 69.2-87.5% (36-41); except for 2 reports, the concordance rates exceeded 80%. However, the tumor grades of endoscopic biopsy specimens and surgical specimens do not always match. The greater the cell number obtained, the better the concordance rate of the NET grade between EUS-FNA specimens and surgical specimens (38). As there is some uncertainty when obtaining a histological specimen by EUS-FNA (36, 38, 39, 42), an endoscopic biopsy through the papilla of Vater was useful for determining the NET grade in the present case. For patients diagnosed with NET G1, a preoperative waiting period may be implemented, or they may only be followed (43). As described above, almost all NEN cases with MPD invasion are high-grade tumors. In addition, in the case reported by Kawakami et al., the patient died 11 months after surgery because of tumor recurrence in the form of multiple liver metastases (Table 2) (12). Therefore, even if the preoperative biopsy specimen indicates a low-grade tumor, early surgery is recommended for NENs with MPD invasion. In another report, MPD involvement was a poor prognostic factor (44). After surgery, patients with PNENs with MPD invasion should be followed closely.

In conclusion, we report the first PNEN case with intraductal growth that was diagnosed by a preoperative endoscopic biopsy through the papilla of Vater. This case is a

good example of a histopathological diagnostic method for pancreatic tumors invading the entire MPD.

The authors state that they have no Conflict of Interest (COI).

References

1. Yao JC, Hassan M, Phan A, et al. One hundred years after "carcinoid": epidemiology of and prognostic factors for neuroendocrine tumors in 35,825 cases in the United States. *J Clin Oncol* **26**: 3063-3072, 2008.
2. Basturk O, Zamboni G, Klimstra DS, et al. Intraductal and papillary variants of acinar cell carcinomas: a new addition to the challenging differential diagnosis of intraductal neoplasms. *Am J Surg Pathol* **31**: 363-370, 2007.
3. Fabre A, Sauvanet A, Flejou JF, et al. Intraductal acinar cell carcinoma of the pancreas. *Virchows Arch* **438**: 312-315, 2001.
4. Hashimoto M, Matsuda M, Watanabe G, et al. Acinar cell carcinoma of the pancreas with intraductal growth: report of a case. *Pancreas* **26**: 306-308, 2003.
5. Iwatate M, Matsubayashi H, Sasaki K, et al. Functional pancreatic acinar cell carcinoma extending into the main pancreatic duct and splenic vein. *J Gastrointest Cancer* **43**: 373-378, 2012.
6. Yang TM, Han SC, Wu CJ, Mo LR. Acinar cell carcinomas with exophytic growth and intraductal pancreatic duct invasion: peculiar multislice computed tomographic picture. *J Hepatobiliary Pancreat Surg* **16**: 238-241, 2009.
7. Yamaguchi H, Shimizu M, Ban S, et al. Intraductal tubulopapillary neoplasms of the pancreas distinct from pancreatic intraepithelial neoplasia and intraductal papillary mucinous neoplasms. *Am J Surg Pathol* **33**: 1164-1172, 2009.
8. Shimizu K, Shiratori K, Toki F, et al. Nonfunctioning islet cell tumor with a unique pattern of tumor growth. *Dig Dis Sci* **44**: 547-551, 1999.
9. Kitami CE, Shimizu T, Sato O, et al. Malignant islet cell tumor projecting into the main pancreatic duct. *J Hepatobiliary Pancreat Surg* **7**: 529-533, 2000.
10. Akatsu T, Wakabayashi G, Aiura K, et al. Intraductal growth of a nonfunctioning endocrine tumor of the pancreas. *J Gastroenterol* **39**: 584-588, 2004.

11. Inagaki M, Watanabe K, Yoshikawa D, et al. A malignant non-functioning pancreatic endocrine tumor with a unique pattern of intraductal growth. *J Hepatobiliary Pancreat Surg* **14**: 318-323, 2007.
12. Kawakami H, Kuwatani M, Onodera M, et al. Primary cholesterol hepatolithiasis associated with cholangiocellular carcinoma: a case report and literature review. *Intern Med* **46**: 1191-1196, 2007.
13. Yazawa N, Imaizumi T, Okada K, et al. Nonfunctioning pancreatic endocrine tumor with extension into the main pancreatic duct: report of a case. *Surg Today* **41**: 737-740, 2011.
14. Hechtman JF, Franssen B, Labow DM, et al. Intraductal polypoid lipid-rich neuroendocrine tumor of the pancreas with entrapped ductules: case report and review of the literature. *Endocr Pathol* **24**: 30-35, 2013.
15. Kiyonaga M, Matsumoto S, Mori H, et al. Pancreatic neuroendocrine tumor with extensive intraductal invasion of the main pancreatic duct: a case report. *JOP* **15**: 497-500, 2014.
16. WHO Classification of Tumours Editorial Board. Digestive System Tumours. In: WHO Classification of Tumours, 5th ed, Vol. 1. World Health Organization, 2019.
17. Cho JH, Ryu JK, Song SY, et al. Prognostic validity of the American joint committee on cancer and the European neuroendocrine tumors staging classifications for pancreatic neuroendocrine tumors: a retrospective nationwide multicenter study in South Korea. *Pancreas* **45**: 941-946, 2016.
18. Pape UF, Jann H, Muller-Nordhorn J, et al. Prognostic relevance of a novel TNM classification system for upper gastroenteropancreatic neuroendocrine tumors. *Cancer* **113**: 256-265, 2008.
19. Yang M, Tian BL, Zhang Y, et al. Evaluation of the World Health Organization 2010 grading system in surgical outcome and prognosis of pancreatic neuroendocrine tumors. *Pancreas* **43**: 1003-1008, 2014.
20. Zeng YJ, Liu L, Wu H, et al. Clinicopathological features and prognosis of gastroenteropancreatic neuroendocrine tumors: analysis from a single-institution. *Asian Pac J Cancer Prev* **14**: 5775-5781, 2013.
21. Lewkowicz E, Trofimiuk-Muldner M, Wysocka K, et al. Gastroenteropancreatic neuroendocrine neoplasms: a 10-year experience of a single center. *Pol Arch Med Wewn* **125**: 337-346, 2015.
22. Yang M, Zeng L, Zhang Y, Su AP, Yue PJ, Tian BL. Surgical treatment and clinical outcome of nonfunctional pancreatic neuroendocrine tumors: a 14-year experience from one single center. *Medicine (Baltimore)* **93**: e94, 2014.
23. Wang YH, Lin Y, Xue L, Wang JH, Chen MH, Chen J. Relationship between clinical characteristics and survival of gastroenteropancreatic neuroendocrine neoplasms: a single-institution analysis (1995-2012) in South China. *BMC Endocr Disord* **12**: 30, 2012.
24. Shiba S, Morizane C, Hiraoka N, et al. Pancreatic neuroendocrine tumors: a single-center 20-year experience with 100 patients. *Pancreatol* **16**: 99-105, 2016.
25. Luo Y, Dong Z, Chen J, et al. Pancreatic neuroendocrine tumours: correlation between MSCT features and pathological classification. *Eur Radiol* **24**: 2945-2952, 2014.
26. Procacci C, Carbognin G, Accordini S, et al. Nonfunctioning endocrine tumors of the pancreas: possibilities of spiral CT characterization. *Eur Radiol* **11**: 1175-1183, 2001.
27. Sahani DV, Bonaffini PA, Castillo CF-D, Blake MA. Gastroenteropancreatic neuroendocrine tumors: role of imaging in diagnosis and management. *Radiology* **266**: 38-61, 2013.
28. Toshima F, Inoue D, Komori T, et al. Is the combination of MR and CT findings useful in determining the tumor grade of pancreatic neuroendocrine tumors? *Jpn J Radiol* **35**: 242-253, 2017.
29. Herwick S, Miller FH, Keppke AL. MRI of islet cell tumors of the pancreas. *AJR Am J Roentgenol* **187**: W472-W480, 2006.
30. Kim DW, Kim HJ, Kim KW, et al. Prognostic value of CT findings to predict survival outcomes in patients with pancreatic neuroendocrine neoplasms: a single institutional study of 161 patients. *Eur Radiol* **26**: 1320-1329, 2016.
31. Tatsumoto S, Kodama Y, Sakurai Y, Shinohara T, Katanuma A, Maguchi H. Pancreatic neuroendocrine neoplasm: correlation between computed tomography enhancement patterns and prognostic factors of surgical and endoscopic ultrasound-guided fine-needle aspiration biopsy specimens. *Abdom Imaging* **38**: 358-366, 2013.
32. Rodallec M, Vilgrain V, Couvelard A, et al. Endocrine pancreatic tumours and helical CT: contrast enhancement is correlated with microvascular density, histoprognostic factors and survival. *Pancreatol* **6**: 77-85, 2006.
33. Guo C, Chen X, Wang Z, et al. Differentiation of pancreatic neuroendocrine carcinoma from pancreatic ductal adenocarcinoma using magnetic resonance imaging: the value of contrast-enhanced and diffusion weighted imaging. *Oncotarget* **8**: 42962-42973, 2017.
34. Suzuki H, Kuwano H, Masuda N, et al. Diagnostic usefulness of FDG-PET for malignant somatostatinoma of the pancreas. *Hepato-gastroenterology* **55**: 1242-1245, 2008.
35. Binderup T, Knigge U, Loft A, et al. Functional imaging of neuroendocrine tumors: a head-to-head comparison of somatostatin receptor scintigraphy, ¹²³I-MIBG scintigraphy, and ¹⁸F-FDG PET. *J Nucl Med* **51**: 704-712, 2010.
36. Larghi A, Capurso G, Carnuccio A, et al. Ki-67 grading of non-functioning pancreatic neuroendocrine tumors on histologic samples obtained by EUS-guided fine-needle tissue acquisition: a prospective study. *Gastrointest Endosc* **76**: 570-577, 2012.
37. Farrell JM, Pang JC, Kim GE, Tabatabai ZL. Pancreatic neuroendocrine tumors: accurate grading with Ki-67 index on fine-needle aspiration specimens using the WHO 2010/ENETS criteria. *Cancer Cytopathol* **122**: 770-778, 2014.
38. Hasegawa T, Yamao K, Hijioka S, et al. Evaluation of Ki-67 index in EUS-FNA specimens for the assessment of malignancy risk in pancreatic neuroendocrine tumors. *Endoscopy* **46**: 32-38, 2014.
39. Unno J, Kanno A, Masamune A, et al. The usefulness of endoscopic ultrasound-guided fine-needle aspiration for the diagnosis of pancreatic neuroendocrine tumors based on the World Health Organization classification. *Scand J Gastroenterol* **49**: 1367-1374, 2014.
40. Fujimori N, Osoegawa T, Lee L, et al. Efficacy of endoscopic ultrasonography and endoscopic ultrasonography-guided fine-needle aspiration for the diagnosis and grading of pancreatic neuroendocrine tumors. *Scand J Gastroenterol* **51**: 245-252, 2016.
41. Sugimoto M, Takagi T, Hikichi T, et al. Efficacy of endoscopic ultrasonography-guided fine needle aspiration for pancreatic neuroendocrine tumor grading. *World J Gastroenterol* **21**: 8118-8124, 2015.
42. Bergeron JP, Perry KD, Houser PM, Yang J. Endoscopic ultrasound-guided pancreatic fine-needle aspiration: potential pitfalls in one institution's experience of 1212 procedures. *Cancer Cytopathol* **123**: 98-107, 2015.
43. Sugimoto M, Takagi T, Suzuki R, et al. Pancreatic neuroendocrine tumor Grade 1 patients followed up without surgery: case series. *World J Clin Oncol* **8**: 293-299, 2017.
44. Nanno Y, Matsumoto I, Zen Y, et al. Pancreatic duct involvement in well-differentiated neuroendocrine tumors is an independent poor prognostic factor. *Ann Surg Oncol* **24**: 1127-1133, 2017.

The Internal Medicine is an Open Access journal distributed under the Creative Commons Attribution-NonCommercial-NoDerivatives 4.0 International License. To view the details of this license, please visit (<https://creativecommons.org/licenses/by-nc-nd/4.0/>).